Editors' Suggestion

Interaction-Induced Crystalline Topology of Excitons

Henry Davenport,[1,*] Johannes Knolle,[2,3,1] and Frank Schindler[1]
[1]Blackett Laboratory, Imperial College London, London SW7 2AZ, United Kingdom
[2]Physics Department, Technical University of Munich, TUM School of Natural Sciences, 85748 Garching, Germany
[3]Munich Center for Quantum Science and Technology (MCQST), Schellingstrasse 4, 80799 München, Germany

(Received 13 June 2024; accepted 18 September 2024; published 21 October 2024)

We apply the topological theory of symmetry indicators to interaction-induced exciton band structures in centrosymmetric semiconductors. Crucially, we distinguish between the topological invariants inherited from the underlying electron and hole bands and those that are intrinsic to the exciton wave function itself. Focusing on the latter, we show that there exists a class of exciton bands for which the maximally localized exciton Wannier states are shifted with respect to the electronic Wannier states by a quantized amount; we call these excitons shift excitons. Our analysis explains how the exciton spectrum can be topologically nontrivial and sustain exciton edge states in open boundary conditions even when the underlying noninteracting bands have a trivial atomic limit. We demonstrate the presence of shift excitons as the lowest energy neutral excitations of the Su-Schrieffer-Heeger model in its trivial phase when supplemented by local two-body interactions.

DOI: 10.1103/PhysRevLett.133.176601

Introduction—The notion of topological insulators has revolutionized our understanding of electronic properties in condensed matter systems [1–3]. Among these, topological crystalline insulators (TCIs) are notable due to their reliance on crystalline symmetries to protect gapless surface and hinge states [4,5]. The classification of TCIs is now quite mature, especially for the subclass of symmetry-indicated topological bands [6–11]. There is therefore now a growing interest in generalizing band topology to incorporate electronic interactions, with particular focus on ground state properties of TCIs in the presence of interactions [12–15].

Excitons are bound states of electrons and holes and, as interaction-induced excitations, are a promising alternative for exploring topological phenomenon in the presence of interactions. This is because the exciton band structure, unlike the band insulating ground state, can be modified substantially even by interactions with characteristic energies much lower than the insulating gap. In this Letter, we apply the topological theory of symmetry indicators to exciton band structures in centrosymmetric semiconductors. A key aspect of our study is distinguishing between topological invariants inherited from electron and hole bands and those intrinsic to the exciton wave function. While previous work has focused on the former (e.g., excitons in Chern bands [16–20]), here we focus on the latter and introduce *shift excitons*, which exhibit maximally localized exciton Wannier states shifted relative to the electronic Wannier states by a quantized amount [21]. We demonstrate nontrivial exciton bands, and exciton edge states, in a simple interaction generalization of the Su-Schrieffer-Heeger (SSH) model with trivial underlying electronic bands.

Theory of shift excitons—We introduce shift excitons for centrosymmetric semiconductors in one dimension (1D). We focus on a spinless two-band tight-binding model at half filling; the definition of shift excitons [e.g., Eq. (5) below] has a straightforward generalization though to n electronic bands in d dimensions. We assume that the occupied band is gapped from the empty band at all momenta and that both bands realize an *unobstructed atomic limit* [8], i.e., their Wannier centers are located at the atomic ions at the unit cell center; this assumption can be relaxed [22]. The electronic bands then have the same inversion $\mathcal{I}$ eigenvalues at both high-symmetry points $k = 0, \pi$ in the 1D Brillouin zone (BZ) if the inversion center is the unit cell center [23]. We study the resulting exciton bands in the presence of interactions.

Let $c_{k,\mathrm{occ}}$ ($c_{k,\mathrm{emp}}$) annihilate an electron in the occupied (empty) band at crystal momentum $k \in [0, 2\pi)$. The noninteracting ground state is given by $|\mathrm{GS}\rangle = \prod_k c^\dagger_{k,\mathrm{occ}}|0\rangle$, where $|0\rangle$ is the fermionic vacuum. The low energy exciton spectrum can be found by projecting the Hamiltonian into the variational exciton basis $c^\dagger_{p+k,\mathrm{emp}} c_{k,\mathrm{occ}}|\mathrm{GS}\rangle$, where p is the total momentum of the electron-hole pair that is

*Corresponding author: h.davenport23@imperial.ac.uk

conserved due to translational symmetry, and k cycles through different relative momenta. An exciton eigenstate with total momentum p takes the form

$$|\phi^p\rangle = \sum_k \phi_k^p c^\dagger_{p+k,\mathrm{emp}} c_{k,\mathrm{occ}} |\mathrm{GS}\rangle, \tag{1}$$

where $\phi_k^p \in \mathbb{C}$ is the exciton wave function. This exciton wave function can describe Frenkel excitons (for ϕ_k^p independent of k) and Wannier-Mott excitons (when ϕ_k^p decays with k) [22,24,25]. The theory of shift excitons applies to both these regimes. We omit the basis state $|\mathrm{GS}\rangle$ in the variational exciton wave function, as its contribution is negligible if the exciton band is sufficiently gapped from the ground state. Crucially, this exciton eigenstate expansion makes it clear that topological invariants can be contributed by the noninteracting Bloch states, which enter the exciton state in Eq. (1) via the electron and hole operators $c^\dagger_{p+k,\mathrm{emp}}$, $c_{k,\mathrm{occ}}$, and/or the exciton wave function itself. We here focus on the exciton wave function to establish a rigorous bulk-boundary correspondence; the bulk topology of the noninteracting electronic bands does not give an exciton bulk-boundary correspondence. This can be seen by considering a 2D system with electronic bands that have a nonzero Chern number. In such a system the Coulomb interaction may give rise to chiral exciton edge states inherited from the electronic edge states [16–20]. However, despite these chiral exciton edge states, the bulk excitons can remain trivial or even gapless and so there is no bulk-boundary correspondence.

As a simple example of intrinsic exciton topology, we investigate the crystalline topology of exciton bands using the symmetry indicators of $\mathcal{I}$ symmetry [6–8,23]. We differentiate between topologically distinct exciton bands using the $\mathcal{I}$ eigenvalues of the exciton states at the high-symmetry points $\tilde{p} = 0, \pi$ of the BZ.

We choose a convenient gauge for the Bloch states $|\psi^{p,\alpha}\rangle$ associated with the underlying noninteracting bands, such that $c^\dagger_{p,\alpha} = \sum_i \langle p, i|\psi^{p,\alpha}\rangle c^\dagger_{p,i}$, $\alpha \in \{\mathrm{occ}, \mathrm{emp}\}$, and $c^\dagger_{p,i}$ creates a Bloch wave with wave vector p on sublattice or orbital i in the unit cell. We adopt the gauge $|\psi^{-p,\alpha}\rangle = \lambda_I^\alpha U_I |\psi^{p,\alpha}\rangle$. Here, the unitary matrix U_I represents $\mathcal{I}$ symmetry in the single-particle Hilbert space, and λ_I^α denotes the $\mathcal{I}$ eigenvalue of the noninteracting band at both high-symmetry points $\tilde{p} = 0, \pi$, which are equal by our assumption of trivial electronic bands.

It follows that $\hat{I} c^\dagger_{p,\alpha} \hat{I}^\dagger = \lambda_I^\alpha c^\dagger_{-p,\alpha}$, where $\hat{I}$ represents $\mathcal{I}$ symmetry in the many-body Hilbert space. Consequently, at $\tilde{p} = 0, \pi$, the $\mathcal{I}$ eigenvalue can be separated into four contributions:

$$\begin{aligned}\hat{I}|\phi^{\tilde{p}}\rangle &= (\lambda_I^{\mathrm{occ}} \lambda_I^{\mathrm{emp}} \lambda_I^{\mathrm{GS}}) \sum_k \phi^{\tilde{p}}_{-k} c^\dagger_{\tilde{p}+k,\mathrm{emp}} c_{k,\mathrm{occ}} |\mathrm{GS}\rangle \\ &\equiv (\lambda_I^{\mathrm{occ}} \lambda_I^{\mathrm{emp}} \lambda_I^{\mathrm{GS}}) \lambda_I^{\mathrm{exc}}(\tilde{p}) |\phi^{\tilde{p}}\rangle. \end{aligned} \tag{2}$$

There are contributions from the $\mathcal{I}$ eigenvalue of the ground state (λ_I^{GS}) as well as the underlying electronic bands. However, the only contribution which varies between different high-symmetry points is the excitonic contribution $\lambda_I^{\mathrm{exc}}(\tilde{p})$ from $\phi_k^{\tilde{p}} = \lambda_I^{\mathrm{exc}}(\tilde{p}) \phi^{\tilde{p}}_{-k}$. We refer to an exciton wave function with $\lambda_I^{\mathrm{exc}}(0) = \lambda_I^{\mathrm{exc}}(\pi)$ as trivial; otherwise it is nontrivial. Nontrivial excitons can therefore arise even in a trivial single-particle band structure, as long as the $\mathcal{I}$ eigenvalues of the exciton wave function differ at $\tilde{p}$. Just like for electronic Wannier states, the Wannier centers of the maximally localized *exciton Wannier states* [21] then shift by a quantized amount [23].

To demonstrate the exciton shift, we define the excitonic Wannier state $|W^{R'}\rangle$ centered at position R', $|W^{R'}\rangle = (1/\sqrt{L}) \sum_p e^{-ipR'} |\phi^p\rangle$. This can be expanded as

$$|W^{R'}\rangle = \sum_{R,\Delta} W_\Delta^{R-R'} c^\dagger_{R,\mathrm{emp}} c_{R-\Delta,\mathrm{occ}} |\mathrm{GS}\rangle. \tag{3}$$

Here, $c^\dagger_{R,\alpha} = (1/\sqrt{L}) \sum_p e^{-ipR} c^\dagger_{p,\alpha}$ are the maximally localized electronic Wannier states associated with the band $\alpha \in \{\mathrm{emp}, \mathrm{occ}\}$ at unit cell R, and

$$W_\Delta^R = \frac{1}{L\sqrt{L}} \sum_{p,k} e^{ipR} e^{ik\Delta} \phi_k^p. \tag{4}$$

We assume that a smooth gauge (as a function of p) has been found for the exciton wave function ϕ_k^p so that the $|W^{R'}\rangle$ (and W_Δ^R) are exponentially localized in space (R); in 1D this is always possible [26]. Note that the spread of W_Δ^R in Δ depends on the electron-hole separation so is greater for Wannier-Mott compared to Frenkel excitons. We define the exciton shift for the exciton Wannier state at unit cell $R' = 0$ as

$$s_{\mathrm{exc}} = \sum_{R,\Delta} |W_\Delta^R|^2 R. \tag{5}$$

While we have so far assumed that the electronic Wannier centers are $x_{\mathrm{occ}} = x_{\mathrm{emp}} = 0$, in general [22],

$$s_{\mathrm{exc}} = \langle W^0|\hat{x}^{(\mathrm{e})}_{\mathrm{emp}}|W^0\rangle - x_{\mathrm{emp}} = \langle W^0|\hat{x}^{(\mathrm{h})}_{\mathrm{occ}}|W^0\rangle - x_{\mathrm{occ}}, \tag{6}$$

where $\hat{x}^{(\mathrm{e})}_{\mathrm{emp}} = \sum_R (R + x_{\mathrm{emp}}) c^\dagger_{R,\mathrm{emp}} c_{R,\mathrm{emp}}$ [$\hat{x}^{(\mathrm{h})}_{\mathrm{occ}} = \sum_R (R + x_{\mathrm{occ}}) c_{R,\mathrm{occ}} c^\dagger_{R,\mathrm{occ}}$] is the empty-band electron (occupied-band hole) projected position operator [26]. Correspondingly, the electron and hole making up the exciton Wannier state are shifted on average by the same amount s_{exc} with respect to the noninteracting electron and hole Wannier centers, respectively. Equivalently, s_{exc} represents the shift with which the actual exciton center of mass is offset from the "naive" exciton center of mass obtained by simply pairing up electron and hole Wannier

states in each unit cell. We next demonstrate that the excitonic shift is quantized to $s_{\mathrm{exc}} = 0, 1/2$ in centrosymmetric systems. $\mathcal{I}$ symmetry requires that $\phi_k^p = e^{i\alpha(p)}\phi_{-k}^{-p}$, where $e^{i\alpha(p)}$ can always be chosen to be a smooth function of p in 1D [23]. The $\mathcal{I}$ eigenvalues at the high-symmetry points constrain $\alpha(p)$. For trivial exciton bands we have $\lambda_I^{\mathrm{exc}}(\tilde{p}) = \lambda_I^{\mathrm{exc}}$, and hence the gauge $\alpha(p)$ can be chosen constant, i.e., $\alpha(p) = \alpha$, where $e^{i\alpha} = \lambda_I^{\mathrm{exc}}$. From Eq. (4), this leads to $W_\Delta^R = \lambda_I^{\mathrm{exc}} W_{-\Delta}^{-R}$ and hence $s_{\mathrm{exc}} = 0$ [22]. However, for nontrivial exciton bands, the $\mathcal{I}$ eigenvalues differ at the high-symmetry points. The required gauge is therefore $\alpha(p) = \alpha - p$, where α is defined via $e^{i\alpha} = \lambda_I^{\mathrm{exc}}(\tilde{p} = 0)$. This gauge choice leads to $W_\Delta^R = \lambda_I^{\mathrm{exc}}(\tilde{p} = 0) W_{-\Delta}^{-(R-1)}$ and hence $s_{\mathrm{exc}} = 1/2$ [22]. Figure 1 demonstrates the difference between shift excitons and trivial excitons and shows explicitly calculated exciton Wannier states for the model introduced in the next section.

A nonzero exciton shift $s_{\mathrm{exc}} = 1/2$ gives a counting mismatch of exciton eigenstates between periodic boundary conditions (PBC) and open boundary conditions (OBC), in analogy to the filling anomaly of obstructed atomic limits [27]. For this, it is crucial to consider an OBC termination that does not cut through any single-particle Wannier states. (Compare this with the usual condition in TCIs that the OBC termination not cut through unit cells.) Given a lattice of N unit cells, there will then be N exciton states that form a band in PBC. If and only if this band has a nontrivial shift $s_{\mathrm{exc}} = 1/2$, it will consist of $N \pm 1$ contiguous exciton states in OBC, potentially (in the case of $N - 1$ states) with 2 midgap exciton states localized at opposite edges of the system. Since these edge states are exponentially localized and exchanged by $\mathcal{I}$ symmetry, they must remain degenerate. In particular, merging them with the bulk excitons does not remove the counting mismatch $N \pm 1 \neq N$ with respect to PBC.

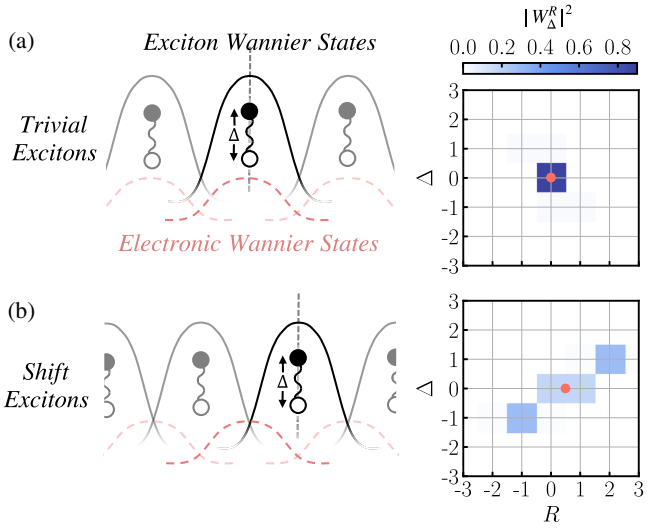

FIG. 1. Conceptual diagram comparing the exciton and electronic Wannier states (in black and red, respectively) for (a) trivial and (b) shift excitons. The right-hand panels show calculated exciton Wannier states for the interacting generalization of the SSH model (introduced in the text) as a function of absolute position R and relative spread Δ. The inversion center for the Wannier states is shown as a red dot, indicating a nontrivial exciton shift $s_{\mathrm{exc}} = 1/2$ for (b).

Shift excitons in the SSH model—Shift excitons can be realized in an interacting generalization of the spinless 1D centrosymmetric SSH model in its trivial phase—that is, there are no single-particle edge states in OBC when terminating with full unit cells. In our conventions, this model has two sublattices labeled A and B and a hopping $(-v)$ between sites within the unit cell and $(-w)$ between adjacent unit cells. $\mathcal{I}$ symmetry inverts about the center of the unit cell, exchanging A and B. The Coulomb interaction introduces quartic terms to the tight-binding Hamiltonian, the form of these is shaped determined by the atomic orbitals. We begin by focusing on the intraunit and interunit cell extended Hubbard interactions, U and U', which are the simplest due to the spinless nature of the model:

$$\begin{aligned}\hat{H} = &-v\sum_R (c_{R,A}^\dagger c_{R,B} + c_{R,B}^\dagger c_{R,A}) \\ &- w\sum_R (c_{R,B}^\dagger c_{R+1,A} + c_{R+1,A}^\dagger c_{R,B}) \\ &+ U\sum_R n_{R,A} n_{R,B} + U'\sum_R n_{R,B} n_{R+1,A}. \end{aligned} \tag{7}$$

We first consider the system in PBC with $v = 1$ and w, U, U' treated perturbatively on top of the noninteracting ground state of the dimerized SSH model (i.e., the ground state at $v = 1$, $w = U = U' = 0$). Since the interunit cell hopping w is zero, there are clearly no edge states in OBC when terminating with full unit cells. Correspondingly, the noninteracting part of the model is in the trivial phase with respect to $\mathcal{I}$ symmetry: since we can localize the sublattices A and B at the center of the unit cell without loss of generality, it realizes an *unobstructed* atomic insulator [8]. This corresponds to an unperturbed ground state $|\mathrm{GS}\rangle = \prod_R c_{R,+}^\dagger |0\rangle$, where $c_{R,+}^\dagger$ is the creation operator for the Wannier state at unit cell R for the filled electronic band. In the dimerized limit, the Wannier states of the occupied $(+)$ and empty $(-)$ bands are compact and localized to a single unit cell [28]:

$$c_{R,\pm}^\dagger = \frac{c_{R,A}^\dagger \pm c_{R,B}^\dagger}{\sqrt{2}}, \qquad \hat{I} c_{R,\pm}^\dagger \hat{I}^\dagger = \pm c_{R,\pm}^\dagger. \tag{8}$$

Excitons consist of excitations of electrons from the occupied Wannier states ($\mathcal{I}$ eigenvalue $+1$) to the empty Wannier states ($\mathcal{I}$ eigenvalue -1). We therefore project the Hamiltonian in Eq. (7) into the variational exciton basis $c_{R+\Delta,-}^\dagger c_{R,+}|\mathrm{GS}\rangle$ to give an effective exciton Hamiltonian

matrix $H_{R,R',\Delta,\Delta'}$. Note we do not include a coupling between the ground state and the exciton basis states because, since we consider w, U, U' perturbatively, the ground state is sufficiently gapped for this coupling to be negligible. The resulting matrix $H_{R,R',\Delta,\Delta'}$ describes the scattering between excitons centered at R, R', with electron-hole separations Δ, Δ'. The Hamiltonian is translationally invariant, $H_{R,R',\Delta,\Delta'} = H_{R-R',0,\Delta,\Delta'}$; hence we perform a Fourier transform resulting in an effective exciton Hamiltonian $H_{\Delta,\Delta'}(p)$ depending on total momentum p,

$$H_{\Delta,\Delta'}(p) = \delta_{\Delta,\Delta'}\Big[2v + U\delta_{\Delta\neq 0} + \frac{U'}{4}(\delta_{\Delta\neq 1} + \delta_{\Delta\neq -1} - 2) - \frac{U'}{2}\delta_{\Delta,0}\cos p\Big] - \frac{w}{2}(\delta_{\Delta',\Delta+1} + \delta_{\Delta',\Delta-1})\Big[1 + e^{ip(\Delta'-\Delta)}\Big], \quad (9)$$

where we have abbreviated $\delta_{\Delta\neq x} \equiv 1 - \delta_{\Delta,x}$. The exciton spectrum above the ground state for the choice $U = U'$ and $w = 0$ is shown in Fig. 2(a) and exhibits a trivial dispersive band of Frenkel excitons ($\Delta = 0$) [22] gapped from a lower set of flat bands (which are doubly degenerate with $\Delta = \pm 1$) and a higher set of flat bands (the electron-hole continuum).

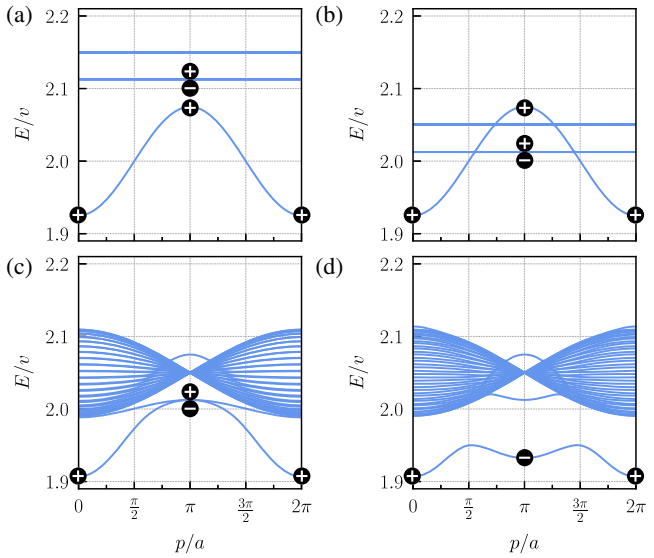

FIG. 2. Construction of a nontrivial exciton band in the interacting SSH model by hybridizing trivial bands. The relevant $\mathcal{I}$ eigenvalues are marked at the high-symmetry momenta. In (a) the lowest energy flat band is twice degenerate so is marked with two $\mathcal{I}$ eigenvalues; the flat band above this is highly degenerate. All spectra have $v = 1$, and the remaining parameters are (a) $U = 0.15$, $U' = 0.15$, $w = 0$, (b) $U = 0.05$, $U' = 0.15$, $w = 0$, (c) $U = 0.05$, $U' = 0.15$, $w = 0.03$, (d) $U = 0.05$, $U' = 0.15$, $w = 0.03$, and pair hopping $V = 0.01$.

To construct a nontrivial exciton band at lowest energy, we begin by lowering the energy of the doubly degenerate flat band by decreasing the interaction strength U with respect to U' [see Fig. 2(b)]. These flat bands hybridize with the dispersive band when the interunit cell hopping term w is turned on. However, this does not result in a nontrivial exciton band (with opposite $\mathcal{I}$ eigenvalues at $p = 0, \pi$) gapped at $p = \pi$ [see Fig. 2(c)]. This can be understood by considering a projected exciton Hamiltonian $H'(p)$ restricted to $\Delta = 1, 0, -1$. The spectrum of this restricted Hamiltonian approximates the low energy physics well because the 3 lowest energy bands in the exciton spectrum are bound states so are exponentially localized in Δ. In the basis $\Delta \in \{1, 0, -1\}$, we obtain

$$H'(p) = \begin{pmatrix} 2v + U - \frac{U'}{4} & -\frac{w}{2}(1 + e^{-ip}) & 0 \\ -\frac{w}{2}(1 + e^{ip}) & 2v - \frac{U'}{2}\cos(p) & -\frac{w}{2}(1 + e^{-ip}) \\ 0 & -\frac{w}{2}(1 + e^{ip}) & 2v + U - \frac{U'}{4} \end{pmatrix}. \quad (10)$$

Clearly, at momentum $p = \pi$, the term multiplying w vanishes, implying that the negative $\mathcal{I}$ eigenstate $(1, 0, -1)^T$ and the positive $\mathcal{I}$ eigenstate $(1, 0, 1)^T$ have the same energy.

Although the gap at $p = \pi$ can be opened using longer-range hopping terms, we aim to not only obtain a nontrivial band gapped at any given momentum, but also to fully gap the nontrivial band across all momenta such that the gap persists in OBC. We show below that when this occurs edge localized excitons can exist. In order for the gap to remain in OBC, however, the highest energy state in the nontrivial band must be lower in energy than all states in the remaining bands. This requirement can never be achieved in the spectrum of the reduced Hamiltonian in Eq. (10), and adding longer-range hopping or further Hubbard-type terms also cannot fully gap the nontrivial band [22].

Generically, however, the Coulomb interaction projected into tight-binding models leads to quartic terms beyond Hubbard-type terms. For example, one can obtain pair hopping terms and these can fully open the gap. Consider, for instance, the pair hopping term

$$\hat{H}_V = V\sum_R (c^\dagger_{R+1,B} c_{R,A} c^\dagger_{R-1,A} c_{R,B} - c^\dagger_{R-1,B} c_{R,A} c^\dagger_{R-1,A} c_{R,B}) + \text{H.c.}, \quad (11)$$

which when projected into the effective 3×3 exciton Hamiltonian adds the term

$$H'_V(p) = \begin{pmatrix} 4V\cos(p) & 0 & -4Ve^{-ip} \\ 0 & 0 & 0 \\ -4Ve^{ip} & 0 & 4V\cos(p) \end{pmatrix}. \quad (12)$$

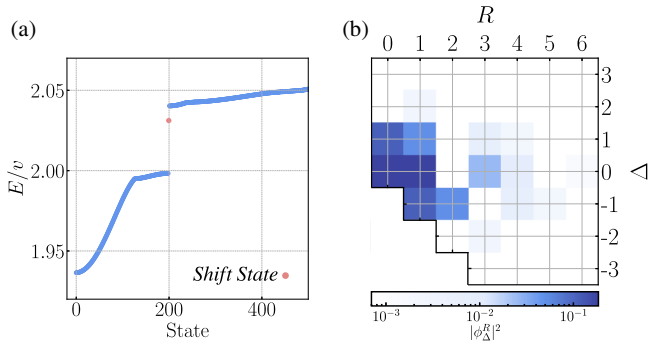

FIG. 3. (a) Spectrum in OBC with the chain terminated on strong bonds (i.e., on a full unit cell when $|v| > |w|$) with $v = 1.0$, $w = 0.03$, $U = 0.1$, $U' = 0.1$, and $V = 0.01$. The exciton states in our variational basis are $\sum_{R,\Delta} \phi^R_\Delta c^\dagger_{R+\Delta,-} c_{R,+}|\mathrm{GS}\rangle$. The mod squared of the wave function ($|\phi^R_\Delta|^2$) for one of the interaction-induced shift exciton edge states [marked Shift State in (a)] is shown in (b). The cutout removes disallowed states (e.g., $\Delta < -R$ is impossible because the left-hand edge of the system is at $R = 0$).

For reasonable parameter choices, this term opens up the gap at all momenta [see Fig. 2(d)]. In addition to being able to gap out a nontrivial exciton band, it can be made completely flat [22], potentially leading to strongly correlated exciton condensate states.

The nontrivial shift $s_{\mathrm{exc}} = 1/2$ of the exciton Wannier centers that follows from their opposite inversion eigenvalues at $\tilde{p} = 0, \pi$ leads to a bulk-boundary correspondence as explained above. We find that when the $|v| > |w|$ chain is terminated with full unit cells (and not cutting through any single-particle Wannier states), there are no edge states in the noninteracting SSH model and yet the interaction-induced nontrivial topology of the exciton bands leads to exciton edge states. Figs. 3(a) and 3(b) show the spectrum and profile of the midgap exciton edge state at the left-hand edge of the chain. These edge states correspond to exciton states which can be excited at the edge and not the bulk; hence the local optical conductivity can be used to detect shift excitons [29–31] (see Ref. [22] for explicit calculations). Note that one can also obtain exciton edge states by terminating the chain on a weak bond (w). This termination can lead to *single-particle* states which have an edge localization which can be inherited by exciton states. However, the resulting exciton edge states differ substantially from those exciton edge states which arise from the bulk exciton topology [22].

Discussion—Our work generalizes the topological classification of TCIs to excitons in semiconductors, paving the way for future explorations into the interplay of topology and interaction-induced bound states in condensed matter systems. Firstly, investigating higher-symmetry groups beyond $\mathcal{I}$ symmetry and applying topological quantum chemistry principles to exciton band structures will uncover new topological phases of excitons. The composite nature of excitons also suggests the possibility of entirely novel topological properties not possible for (quasi)electrons. Additionally, the condensation of shift excitons might lead to a new state of matter, termed a shift-excitonic insulator, with unique collective excitations and phase transitions. Finally, our approach can be naturally generalized to other excitations, such as plasmons, magnons, polarons, magnon-magnon pairs, and triplons.

Note added—Recently, Ref. [32] appeared, where it is suggested that organic semiconductors may realize shift excitons.

Acknowledgments—We thank Gaurav Chaudhary, Julian May-Mann, and Ryan Barnett for inspiring discussions. We acknowledge support from the Imperial-TUM flagship partnership. H. D. acknowledges support from the Engineering and Physical Sciences Research Council (Grant No. EP/W524323/1). J. K. acknowledges support from the Deutsche Forschungsgemeinschaft (DFG, German Research Foundation) under Germany's Excellence Strategy–EXC–2111–390814868, DFG Grants No. KN1254/1-2, No. KN1254/2-1, and No. TRR 360–492547816, as well as the Munich Quantum Valley, which is supported by the Bavarian state government with funds from the Hightech Agenda Bayern Plus. This work was performed in part at Aspen Center for Physics, which is supported by National Science Foundation Grant No. PHY-2210452.

[1] M. Z. Hasan and C. L. Kane, Rev. Mod. Phys. **82**, 3045 (2010).
[2] C. L. Kane and E. J. Mele, Phys. Rev. Lett. **95**, 226801 (2005).
[3] B. A. Bernevig and S.-C. Zhang, Phys. Rev. Lett. **96**, 106802 (2006).
[4] L. Fu, Phys. Rev. Lett. **106**, 106802 (2011).
[5] R.-J. Slager, A. Mesaros, V. Juričić, and J. Zaanen, Nat. Phys. **9**, 98 (2013).
[6] J. Kruthoff, J. de Boer, J. van Wezel, C. L. Kane, and R.-J. Slager, Phys. Rev. X **7**, 041069 (2017).
[7] H. C. Po, A. Vishwanath, and H. Watanabe, Nat. Commun. **8**, 50 (2017).
[8] B. Bradlyn, L. Elcoro, J. Cano, M. G. Vergniory, Z. Wang, C. Felser, M. I. Aroyo, and B. A. Bernevig, Nature (London) **547**, 298 (2017).
[9] Z. Song, S.-J. Huang, Y. Qi, C. Fang, and M. Hermele, Sci. Adv. **5**, eaax2007 (2019).
[10] K. Shiozaki, M. Sato, and K. Gomi, Phys. Rev. B **106**, 165103 (2022).
[11] N. Wagner, L. Crippa, A. Amaricci, P. Hansmann, M. Klett, E. J. König, T. Schäfer, D. D. Sante, J. Cano, A. J. Millis, A. Georges, and G. Sangiovanni, Nat. Commun. **14**, 7531 (2023).
[12] M. O. Soldini, N. Astrakhantsev, M. Iraola, A. Tiwari, M. H. Fischer, R. Valentí, M. G. Vergniory, G. Wagner, and T. Neupert, Phys. Rev. B **107**, 245145 (2023).

[13] K. Shiozaki, C. Z. Xiong, and K. Gomi, Prog. Theor. Exp. Phys. **2023**, 083I01 (2023).
[14] N. Manjunath, V. Calvera, and M. Barkeshli, Phys. Rev. B **109**, 035168 (2024).
[15] J. Herzog-Arbeitman, B. A. Bernevig, and Z.-D. Song, Nat. Commun. **15**, 1171 (2024).
[16] K. Chen and R. Shindou, Phys. Rev. B **96**, 161101(R) (2017).
[17] Z. R. Gong, W. Z. Luo, Z. F. Jiang, and H. C. Fu, Sci. Rep. **7**, 42390 (2017).
[18] H.-Y. Xie, P. Ghaemi, M. Mitrano, and B. Uchoa, Proc. Natl. Acad. Sci. U.S.A. **121**, e2401644121 (2024).
[19] Y. H. Kwan, Y. Hu, S. H. Simon, and S. A. Parameswaran, Phys. Rev. Lett. **126**, 137601 (2021).
[20] A. Blason and M. Fabrizio, Phys. Rev. B **102**, 035146 (2020).
[21] J. B. Haber, D. Y. Qiu, F. H. da Jornada, and J. B. Neaton, Phys. Rev. B **108**, 125118 (2023).
[22] See Supplemental Material at http://link.aps.org/supplemental/10.1103/PhysRevLett.133.176601 for details on the general definition of Shift excitons, SSH model calculations, and experimental probes.
[23] A. Alexandradinata, X. Dai, and B. A. Bernevig, Phys. Rev. B **89**, 155114 (2014).
[24] P. Anderson, *Concepts in Solids: Lectures on the Theory of Solids*, Advanced Book Classics Series (World Scientific, Singapore, 1997).
[25] I. Egri, J. Phys. C **12**, 1843 (1979).
[26] N. Marzari and D. Vanderbilt, Phys. Rev. B **56**, 12847 (1997).
[27] W. A. Benalcazar, T. Li, and T. L. Hughes, Phys. Rev. B **99**, 245151 (2019).
[28] F. Schindler and B. A. Bernevig, Phys. Rev. B **104**, L201114 (2021).
[29] R. Kubo, J. Phys. Soc. Jpn. **12**, 570 (1957).
[30] F. Wu, T. Lovorn, and A. H. MacDonald, Phys. Rev. Lett. **118**, 147401 (2017).
[31] Y. Luo, R. Engelke, M. Mattheakis, M. Tamagnone, S. Carr, K. Watanabe, T. Taniguchi, E. Kaxiras, P. Kim, and W. L. Wilson, Nat. Commun. **11**, 4209 (2020).
[32] W. J. Jankowski, J. J. P. Thompson, B. Monserrat, and R.-J. Slager, arXiv:2406.11951.